TR/102 December 1980

Two Numerical Methods for the Conformal Mapping of Simply-Connected Domains

by

N. Papamichael and C.A. Kokkinos*

* On study leave from the National Technical University of Athens.

SUMMARY

Two numerical methods are considered for the conformal mapping of a bounded simply-connected domain onto the unit disc. The two methods are respectively the Bergman kernel method, which has been described in [17], and the so-called Ritz method. In this paper we indicate the close theoretical relationship of the two methods, compare their computational efficiencies and present a number of practical applications of the approximate conformal maps.

1. Introduction

Let Ω be a bounded simply-connected domain in the complex z-plane, and let $w = f(z)$ be the function which maps conformally Ω onto the disc $|w| < R$. In this paper we consider the problem of determining numerical approximations to the mapping function f. More specifically, we consider two closely related methods which lead to approximations of the form

$$f_n(z) = \sum_{j=1}^{n} a_j u_j(z) \quad , \tag{1.1}$$

where $\{u_j\}$ is an appropriate set of basis functions. One of these two methods is the Bergman kernel method (BKM), proposed recently by Levin, Papamichael and Sideridis [17]. The other method is the so-called Ritz method (RM).

The RM is a variational method, based on the "property of minimum area", i.e. the property that the derivative f of the mapping function f minimizes the integral

$$\iint_{\Omega} |u(z)|^2 \, dxdy \tag{1.2}$$

over a certain class of analytic functions. In this method the coefficients a_j of the approximation (1.1), are determined by solving an (n-1) x (n-1) complex linear system with a Gram matrix of coefficients. The BKM is based on the use of the so-called Bergman kernel function of Ω. This kernel function is closely related to the function f' which minimizes (1.2) and, for this reason, the RM and BKM can be regarded as being theoretically equivalent. However, in the BKM the approximation (1.1) is obtained by constructing a Fourier series representation of the kernel function, and the coefficients a_j are determined by means of an orthonormalization procedure. Thus, the two methods are computationally different.

The theory of the two methods is treated extensively in the literature;

see e.g. [2], [10], [19], [20] and [31]. In particular, Gaier [10] considers fully not only the theory but also the numerical implementation of the two methods. However, the numerical methods of [10] involve the use of a polynomial basis set $\{u_j\}$ and, in many cases, such a basis does not lead to approximations of acceptable accuracy. In the present paper the basis set, for both the RM and the BKM, is selected by using the procedure proposed, in connection with the BKM, in [17]. This procedure leads to a non-polynomial basis set, which includes terms that reflect the main singular behaviour of f in the complement of Ω.

The objectives of the present paper are as follows. To indicate the close theoretical relationship between the BKM and the RM, to present the computational details of the RM and to compare the computational efficiencies of the two methods. The motivation for such a comparison emerges from the results contained in [10,p. 154], which suggest that the RM is substantially faster than the BKM. Our numerical experiments show that the two methods require the same computational effort for producing approximations of comparable accuracy. These experiments also show that both the BKM and the RM can be used to produce approximations of high accuracy. The essential requirement for this is that the basis set includes appropriate "singular" functions.

In addition to the objectives stated above, another major purpose of the present paper is to consider certain practical applications of the approximate conformal maps. In particular, we show that these approximate maps can be used to produce, with very little additional computational effort, accurate approximations to the moduli of a class of doubly-connected domains.

2. The Property of Minimum Area

Let Ω be a bounded simply-connected domain with boundary $\partial\Omega$ in the complex z-plane ($z = x+iy$), and assume, without loss of generality, that the origin 0 is in Ω. Also, let

$$w = f(z) \quad , \tag{2.1}$$

be the mapping function which maps Ω conformally onto the disc,

$$D_R = \{w:|w|<R\} \quad ,$$

in such a way that $f(0) = 0$ and $f'(0) = 1$. The radius R of the disc is called the conformal radius of the mapping.

It is well-known that the space of all square integrable analytic functions in Ω is a Hilbert space with inner product

$$(g_1, g_2) = \iint_\Omega g_1(z)\overline{g_2(z)}\,dxdy \tag{2.2}$$

see e.g. [32;p53], We denote this space by $L_2(\Omega)$ and let

and

$$K^{(1)}(\Omega) = \{u(z):u\in L_2(\Omega) \text{ and } u(0) = 1\} \quad ,$$

$$K^{(0)}(\Omega) = \{v(z):v\in L_2(\Omega) \text{ and } v(0) = 0\} \quad .$$

The theory on which the two numerical methods are based emerges by considering the following variational problem.

Problem 2.1. To minimize

$$\|u\|^2 = \iint_\Omega |u(z)|^2\,dxdy \quad , \tag{2.3}$$

over all $u\in K^{(1)}(\Omega)$.

The following results hold:

R 2.1 Problem 2.1 has a unique solution u_0 .

R 2.2 The minimal function u_n is related to the mapping function f by

$$u_0(z) = f'(z). \tag{2.4}$$

R 2.3 The minimum of (2.3) is equal to the area of the disc D_R, i.e.

$$\|u_0\|^2 = \pi R^2 \tag{2.5}$$

R 2. 4 The minimal function u_0 is orthogonal to every function $v \in K^{(0)}(\Omega)$, i.e.

$$(u_0, v) = 0, \qquad \forall\, v \in K^{(0)}(\Omega). \tag{2.6}$$

R 2.5 The space $L_2(\Omega)$ has a unique reproducing kernel $K(z;0)$ such that

$$g(0) = (g, K), \qquad \forall\, g \in L_2(\Omega), \tag{2.7}$$

and this kernel is related to the minimal function u_0 by

$$K(z;0) = u_0(z) / ||u_0||^2. \tag{2.8}$$

Since $K^{(1)}(\Omega)$ and $K^{(0)}(\Omega)$ are respectively a closed convex subset and a closed subspace of $L_2(\Omega)$, the results R2.1 and R2.4 are direct consequences of two standard results of the theory of Hilbert spaces; see e.g. Pryce [25;p.p.168-69]. Alternatively, R2.1, R2.4 and also R2.2 and R2.3 can be established by making use of the properties of the mapping function f; see e.g. Gaier [10,p.118] and Walsh [31,p.322]. Finally, R2.5 follows from the theory of reproducing kernels of Aronszajn [1], by observing that if $|z - z_0| \leq r$ lies entirely within Ω then

$$|g(z_0)|^2 \leq \frac{1}{\pi r^2} ||g||^2, \quad \forall\, g \in L_2(\Omega) \tag{2.9}$$

see [1,p,343] and, for a proof of (2.9), [10,p.117].

The results R2.1 - R2.3 constitute the well-known property of minimum area of Bieberbach [4]. The kernel K(z;0) of (2.8) is known as the Bergman kernel function of Ω. Its properties and its application to conformal mapping mapping are studied fully in [2].

3. Numerical Methods

The theoretical results of Section 2 lead to the following two numerical methods for determining approximations to the mapping function f.

3.1 The Ritz Method This method emerges by seeking the solution of the finite-dimensional counterpart of Problem 2.1

Let $\{n_j(z)\}$ be a complete set of $L_2(\Omega)$ and denote by $K_n^{(1)}(\Omega)$ and $K_n^{(0)}(\Omega)$

the n-dimensional counterparts of $K^{(1)}(\Omega)$ and $K^{(0)}(\Omega)$ corresponding to the set $\{n_j.(z)\}$, i.e.

$$K_n^{(1)}(\Omega) = \left\{ \phi_n(z):\ \phi_n = \sum_{j=1}^{n} c_j \eta_j,\ c_j \in \mathbb{C} \text{ and } \phi_n(0) = 1 \right\},$$

and

$$K_n^{(0)}(\Omega) = \left\{ \psi_n(z):\ \psi_n = \sum_{j=1}^{n} d_j \eta_j,\ c_j \in \mathbb{C} \text{ and } \psi_n(0) = 0 \right\},$$

Then the finite-dimensional variational problem corresponding to Problem 2.1 can be stated as follows.

Problem 3.1 To minimize

$$||\phi_n||^2 = \iint_\Omega |\phi_n(z)|^2 \, dxdy \quad , \tag{3.1}$$

over all $\phi_n \in K_n^{(1)}(\Omega)$.

The following results hold:

R 3.1 Problem 3.1 has a unique solution $\hat{\phi}_n$.

R 3.2 The minimal function $\hat{\phi}_n$ is completely characterized by the property

$$(\hat{\phi}_n, \psi_n) = 0, \qquad \forall\ \psi_n \in K_n^{(0)}(\Omega)$$

R 3.3 The minimal function $\hat{\phi}_n$ converges almost uniformly in Ω to $u_0 = f'$. (By almost uniform convergence we mean convergence in every closed subdoraain of Ω.)

The results R3.1 and R3.2 are the finite-dimensional counterparts of R2.1 and R2.4. Like R2.1 and R2.4, they are particular cases of standard results from the theory of Hilbert spaces. The theory of Hilbert spaces also shows that $\hat{\phi}_n$ converges to u_0 in the norm of $L_2(\Omega)$. The result R3.3 is a direct consequence of the fact that in $L_2(\Omega)$ convergence in the norm implies almost uniform convergence; see e.g. Simirnov and Lebedev [27,p.209].

To determine an approximation $f_n(z)$ to f(z) we proceed as follows. We choose the set $\{\eta_j(z)\}$ so that

$$\eta_1(0) = 1 \text{ and } \eta_j(0) = 0;\ j = 2,3,\ldots, \tag{3.2}$$

and let

$$\phi_n(z) = \eta_1(z) = \sum_{j=2}^{n} c_j u_j(z) \quad , \tag{3.3}$$

Then, from R3. 2, the n^{-1} complex coefficients c_j must be determined so that

$$(\hat{\phi}_n, \psi_n) = 0 \qquad \forall\ \psi_n \in K_n^{(0)}(\Omega)\,. \tag{3.4}$$

Because of the choice (3.2) of the n_j, any function $\psi_n \in K_n^{(0)}(\Omega)$ has an expansion of the form

$$\psi_n(z) = \sum_{j=2}^{n} d_j \eta_j(z) \quad ,$$

This implies that a necessary and sufficient condition for (3.4) to hold is

$$(\hat{\phi}_n, n_i) = 0 \ ; \qquad i = 2,3,.....,n.$$

or

$$(\eta_1, \eta_i) + \sum_{j=2}^{n} c_j (\eta_j, \eta_i) = 0 \ ; \qquad i = 2,3,.....,n. \tag{3.5}$$

The equations (3.5) constitute an (n-l)x(n-l) complex linear system with a Gram matrix of coefficients. Thus, the matrix in (3.5) is Hermitian and positive definite.

The system (3.5) is solved for the unknown coefficients c_j in (3.3) and then, from R3.3,

$$f_n(z) = \int_{\cap}^{z} \hat{\phi}_n(\varsigma)\, d\varsigma \quad , \tag{3.6}$$

gives an approximation to the mapping function f. Also, from (2.3),

$$R_n \,||\hat{\phi}_n||\,/\sqrt{\pi} \tag{3.7}$$

gives an approximation to the radius R of the disc D_R. This implies that

$$F_n(z) = \left\{\sqrt{\pi} \int_0^z \hat{\phi}_n(\varsigma\, d\varsigma\right\}/||\hat{\phi}_n|| \quad , \tag{3.8}$$

gives an approximation to the function F which maps conformally Ω onto the unit disc D_1 in such a way that $F(0) = 0$ and $F'(0)>0$.

We shall refer to the above method of numerical conformal mapping as the Ritz method (RM) with basis $(n_j(z))$.

3.2 The Bergman Kernel Method. The mapping function f is related to the Bergman kernel function of Ω by

$$f(z) = \left\{ \int_0^z K(\varsigma\ ;\ 0)\, d\varsigma\right\}/K(0,0) \tag{3.9}$$

This follows at once from (2.4) and (2.8), by observing that

$$K(0,0) = 1/||\mu_0||^2. \tag{3.10}$$

In the Bergman kernel method the approximation to f is determined from (3.9), by first approximating the kernel K(z;0) by a finite Fourier series sum.

Let $\{\eta_j^*(z)\}$ be a complete orthonormal set of $L_2(\Omega)$ and consider the Fourier series expansion of K(z;0). Because of the reproducing property (2.7), the Fourier coefficients are

$$(K,n_j^*) = \overline{n_j^*(0)}.$$

Thus, the kernel has the infinite series expansion

$$K(z;0) = \sum_{j=1}^{\infty} \overline{\eta_j^*(0)}\,\eta_j^*(z) \quad , \tag{3.11}$$

which certainly converges in the norm of $L_2(\Omega)$. Furthermore, as in the case of R3.3, this norm convergence implies that (3.11) converges almost uniformly in Ω.

Given a complete set $\{n_j(z)\}$ of $L_2(\Omega)$, the results (3.9) and (3.11) suggest the following procedure for obtaining a numerical approximation to the mapping function f. The set $\{nj(z)\}_{j=1}^{n}$. is orthonormalized by means of the Gram-Schmidt process to give the set of orthonormal functions $\{n_j^*(z)\}_{j=1}^{n}$. The series (3.11) is then truncated after n terms to give the approximation

$$K_n(z;0) = \sum_{j=1}^{n} \overline{\eta_j^*(0)}\,\eta_j^*(z) \quad , \tag{3.12}$$

to K(z;0) and finally equation (3.9) is used to give the approximation

$$f_n(z) = \{K_n(0,0)\}^{-1} \int_0^z K_n(\varsigma;0)\, d\varsigma \quad , \tag{3.13}$$

to the mapping function f. Also, from (2.3) and (3.10),

$$R_n = \{\pi K_n(0,0)\}^{-1/2} \quad , \tag{3.14}$$

is an approximation to the radius R of the disc. Thus,

$$F_n(z) = \left\{\frac{\pi}{K_n(0,0)}\right\}^{-1} \int_0^z K_n(\varsigma;0)\, d\varsigma \quad , \tag{3.15}$$

gives an approximation to the function F which maps Ω conformally onto the unit disc D_1.

We shall refer to the above method of numerical conformal mapping as the Bergman Kernel method (BKM) with basis $\{n_j(z)\}$.

4. Choice of Basis

Both the RM and the BKM lead to approximations of the form

$$f_n(z) = \sum_{j=1}^{n} a_j u_j(z) \quad , \tag{4.1}$$

where the u_j are integrals of the basis functions n_j. In the RM the coefficients a_j are derived from the solution of the linear system (3.5), whilst in the BKM the determination of the a_j involves the use of the Gram-Schmidt process- Unfortunately both these methods for determining the a_j may lead to a significant loss of accuracy, due to ill-conditioning of the matrix in (3.5) or to numerical instability of the Gram-Schmidt process; see Svecova[28] and Davis and Rabinowitz [9;p.61]. Thus, in practice, only a limited number of terms in the series approximation to f can be computed accurately. This implies that the success of either the RM or the BKM depends strongly on the speed with which the approximating series converges. Since this convergence depends on the set of basis functions used, it follows that the choice of an appropriate basis is of paramount practical importance.

A computationally convenient basis is the set of monomials

$$n_j(z) = z^{j-1} \quad ; \qquad j = 1,2, \ldots\ldots \tag{4.2}$$

This set is complete in $L_2(\Omega)$ provided that Ω is a Caratheodory domain, i.e. provided that Ω is also the boundary of the complement $\overline{\Omega}^c$ of $\overline{\Omega} = \Omega \cup \partial\Omega$; see e.g. [2,p.14] and [19;p.38,p.117].

The use of (4.2) as basis for the BKM is considered by Bergman and Herriot [3], Burbea [6] and, for both the RM and the BKM, by Gaier[10]. Unfortunately, the convergence of the resulting polynomial approximations is often extremely slow and, for this reason, the **use** of (4.2) as basis does not

lead to a practical method for numerical conformal mapping.

The use of the BKM is also considered by Levin, Papamichael and Sideridis [17]. They observe that the slow convergence of the polynomial approximations is due to the presence of singularities of the mapping function f in the complement Ω^c, of Ω. They also observe that, in many cases, considerable information about these singularities is available and, by using this information, they construct a non-polynomial basis for which the series (3.11) converges rapidly. More specifically the method of Levin et al [17], for constructing a basis for the BKM, is to augment the monomial set (4.2) by introducing functions which reflect the main singular behaviour of the kernel $K(z;0)$. Naturally, the same procedure can be used to obtain an appropriate augmented basis for the RM.

The singular functions needed for augmenting the set (4.2) are determined by considering the poles and branch point singularities of the mapping function f as follows:

4,1 Poles Let the mapping function f have a simple pole at a point $p \in \overline{\Omega}^c$. Then, since

$$u_0(z) = f'(z), \quad K(z;0) = K(0,0)f'(z) \text{ and } f(0) = 0, \tag{4.3}$$

in order to remove the influence of this pole from the numerical process we augment the set (4.2) by introducing the function

$$\begin{aligned} \eta(z) &= \{z/(z-p)\}' + c \\ &= \{-p/(z-p)^2\} + c \ , \end{aligned} \tag{4.4}$$

where $c = 1/p$ in the case of the RM, and $c = 0$ in the case of the BKM. (The reason for including the constant c in (4.4) is that in the RM the basis functions must satisfy the conditions (2.2).) The basis is constructed in this way be considering only the poles of f that lie close to the boundary $\partial\Omega$ Thus, the procedure of [17] for constructing a basis requires knowledge of the dominant poles of f. This knowledge is often available through the Green's function $G(x,y;0)$ of Ω which is connected to f by

$$f(z) = \exp\{-27\pi(G(x,y;0) + iH(x,y))\}, \tag{4.5}$$

where H is the harmonic conjugate of G.

Let G have a singularity of the form

$$\{\log |z-p| \}/2\pi \quad , \tag{4.6}$$

at the point $p \in \overline{\Omega}^c$. Then, it follows from (4.5) that f has a simple pole at p. This shows that the construction of the augmented basis requires knowledge of the dominant singularities of the Green's function of Ω, in the complement of $\overline{\Omega}$. For polygonal domains, and for domains whose boundaries consist of straight line segments and circular arcs, these singularities can be determined by the method of images; see [17;p.175] and also Copson [8;p.150]. For domains involving more general boundaries no standard technique for determining the dominant singularities of G, and hence the corresponding poles of f, is available. However, as is observed in [17], if a good approximation $\tilde{p}$ to the pole at $z=p$ can be obtained, by some method, then the introduction of the function

$$\{- \tilde{p} /(z- \tilde{p})^2\} + c$$

into the set (4.2) is sufficient to remove the influence of the pole from the numerical process.

4.2 Branch Point Singularities. Let Ω be partly bounded by two analytic arcs Γ_1 and Γ_2 which meet at a point z_0 and form there a corner of interior angle air, where $a = p/q$ is a fraction reduced to lowest terms. We consider the asymptotic behaviour of the mapping function f in the neighbourhood of z_0 .

If Ω is a polygonal domain then the Schwarz-Christoffel formula shows that, in the neighbourhood of z_0 ,

$$f(z) - f(z_0) \sum_{k=1}^{\infty} a_k (z-z_0)^{k/\alpha},$$

or since f(0) - 0,

$$f(z) = \sum_{k=1}^{\infty} a_k \{(z - z_0)^{k/\alpha} - (-z_0)^{k/\alpha}\} \quad , \tag{4.7}$$

where $a_1 \neq 0$; see e.g. Copson [8;p.170]. This shows that unless $1/\alpha$ is an integer f has a branch point singularity at z , due to the presence of

fractional powers of $(z-z_0)$ in (4.7). In order to remove the influence of such a singularity from the numerical process, we follow the procedure of [17] and augment the set (4.2) by introducing the functions

$$\eta(z) = \left\{(z-z_0)^{k/\alpha} - (-z_0)^{k/\alpha}\right\} - d$$

$$= \frac{k}{\alpha}(z-z_0)^{k/\alpha-1} - d \qquad (4.8)$$

corresponding to the first few singular terms of (4.7). In (4.8), $d = \left\{k(-z_0)^{k/\alpha-1}\right\}/\alpha$ in the case of the RM, and $d = 0$ in the case of the BKM.

If Ω is a non-polygonal domain then the singular functions required for the augmentation of (4.2) can be determined from the asymptotic expansion

$$f(z) - f(z_0) = \sum_{k,\ell,m,} B_{k,\ell,m,}(z-z_0)^{k,\ell,/\alpha}(\log(z-z_0))^m \ , \qquad (4.9)$$

which is due to Lehman [16]. In (4.9), $k = 0,1,2,\ldots\ldots\ldots\ldots$, $1 \le \ell \le p$, $0 \le m \le k/q$, $B_{0,1\,0} \neq 0$, and the term corresponding to $B_{k,\ell,m}$ precedes the term corresponding to $B_{k',\ell',m'}$ if either $k + \ell/a < k' + \ell'/\alpha$ or $k+\ell/\alpha = k'+\ell'/\alpha$ and $m > m'$.

We note that (4.9) differs from (4.7) in that apart from powers of $(z-z_0)$ it also involves terms of the form

$$(z-z_0)^{\beta}\{\log(z-z_0)\}^m \ , \qquad (4.10)$$

where m is an integer. This implies that for a non-polygonal domain, we cannot conclude that there is no singularity at z_0 even when $1/\alpha$ is an integer.

5. Computational Details and Numerical Examples.

In all the examples considered in this section we compute approximations to the mapping function F which maps conformally Ω onto the unit disc D_1. Thus, in the case of the RM the approximation F_n is determined from (3 3) and (3.8), and in the case of the BKM from (3.12) and (3.15).

The evaluation of the coefficients of the linear system (3.5) and the orthonormalization of the set $\{n_j(z)\}$ by means of the Gram-Schmidt process

require the computation of the inner products

$$(\eta_r , \eta_s) = \iint_\Omega \eta_r (z) \overline{\eta_s (z)} \, dxdy \; ; \quad r, s = 1,2 ,\ldots, n \; .$$

Using a Green's formula ([10,p. 118], [20,p.240]), the inner products are expressed in the form

$$(\eta_r , \eta_s) = \frac{1}{2i} \int_{\partial\Omega} \eta_r (z) \overline{\mu_s (z)} dz \; \mu_s' (z) = \eta_s (z), \tag{5.1}$$

and the integrals in (5.1) are computed, as proposed in [17,p.177], by Gaussian quadrature. If, due to the presence of a corner, the basis set contains functions of the form (4.8) or (4.10) then the Gauss-Legendre formula may fail to produce sufficiently accurate approximations to the inner products which involve these singular functions. It is then necessary to use special techniques in order to imporve the accuracy of the quadrature. These techniques depend on the geometry of $\partial\Omega$ and, for this reason, it is not possible to describe a procedure for a general $\partial\Omega$. If however, as is frequently the case, the arms Γ_1 , Γ_2 of the corner z_0 are both straight line segments then the singularities of the integrands can always be removed, quite simply, by choosing an appropriate parametric representation for $\partial\Omega$; see [17,p.177] for further details.

In the RM the complex linear system (3.5) is solved by using the NAG Library routines F01BN and F04AW. These routines compute the solution of (3.5), by applying Cholesky's method on the positive definite Hermitian matrix of coefficients. The orthonormalization procedure used in the BKM is based on the standard Gram-Schmidt algorithm; see e.g. [9,p.67] and [6,p.822].

An estimate of the maximum error in $|F_n(z)|$ is given by the quantity E_n. This is obtained, as described in [17], by computing

$$e_n(z) = 1 - |F_n(z)| \quad , \tag{5.2}$$

at a number of "boundary test points" $z_j \in \delta\Omega$ and then determining

$$E_n = \max_j |e_n (z_j)| \; . \tag{5.3}$$

In each example, the BKM results presented correspond to the approximation $F_{N_{opt}}$, where $n = N_{opt}$ is the "optimum number" of basis functions which gives maximum accuracy in the sense explained in [17, p. 177]. That is, this number is determined by computing a sequence of approximations $\{F_n(z)\}$, where at each stage the number n of basis functions is increased by one. If at the $(n+1)^{th}$ stage the inequality

$$E_{n+1} < E_n \quad , \tag{5.4}$$

is satisfied then the approximation F_{n+2} is computed. When for a certain value of n, due to numerical instability, (5.4) no longer holds then we terminate the process and take $n = N_{opt}$

In the case of the RM the above procedure for determining N_{opt} is computationally expensive, since for each new value of n the determination of F_n requires the solution of a new (n-1)x(n-1) complex linear system. For this reason, in each example, the RM approximations correspond to $n = N_{opt}$, where N_{opt} is the optimum value of n used in the BKM. It should be observed that if the number of basis functions is increased above a certain value n our RM procedure fails. This failure is due to our choice of subroutines for the solution of the linear system (3.5) and occurs when, due to the accumulation of rounding errors, the matrix of (3.5) ceases to be positive definite. We do not regard this as a drawback of the method, since such a failure serves as a warning of ill-conditioning and indicates that the value of n should be decreased.

In presenting the results we adopt the notation used in [17] and denote the BKM with monomial basis (4.2) by BKM/MB and the BKM with augmented basis by BKM/AB. Similarly. we denote the corresponding RM methods by RM/MB and RM/AB. For each example we list the singular functions used for augmenting (4.2), the boundary test points and the order of the Gaussian quadrature used. Also, when the accurate computation of the inner products requires the use of a special parametric representation for part of the boundary $\partial\Omega$, we give this representation. In each case

the numerical results presented are values of E_{Nopt} obtained, as described above, by using (5.3). We also present the computed values R_{Nopt}, approximating the conformal radius R. These approximations are computed, in the case of the RM., from (3.7) and, in the case of the BKM, from (3.15). The domains in the three examples considered below are chosen because they are needed for the applications contained in Section 6. Several other geometries, illustrating the application of the BRM and the considerable improvement in accuracy obtained by using the BKM/AB instead of the BKM/MB, are considered in [17]. Also, the explicit BKM/AB formulae for the approximate conformal mapping of several domains can be found in [21]. All computations were carried out, in single length arithmetic, on a CDC 7600 computer.

Example 5.1 Quadrilateral; Figure 5.1.

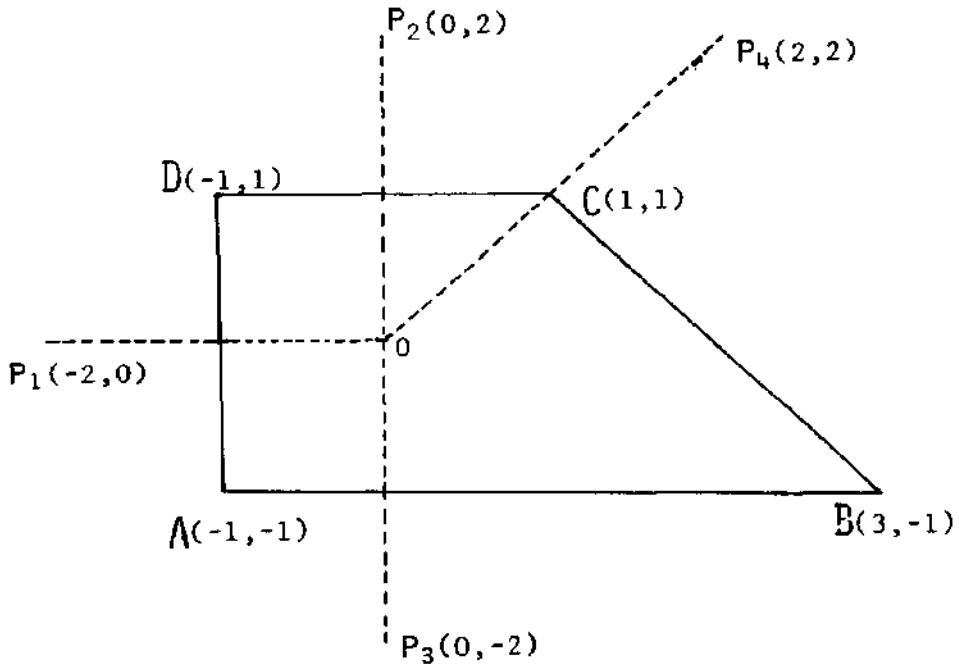

FIGURE 5.1

Augmented Basis. The following singular functions, corresponding respectively to the poles at the points p_j ; j = 1,2,3,4 and the branch point singularity

at the corner C = z_C are used: $-p_j/(z-p_j)^2 + c_j$; j = 1,2,3,4 and $\frac{4k}{3}(z-z_C)^{\frac{4k}{3}-1} - d_k$; k = 1, 2, where in the BKM/AB $c_j = 0$, $d_k = 0$ and in the RM/AB, $c_j = 1/P_j$, $d_k = \left\{4k(-z_C)^{\frac{4k}{3}-1}\right\} / 3.$

Quadrature. Gauss -Legendre formula with 16 points along each side of the polygon.

In order to perform the integration accurately we choose the parametric representations of BC and CD to be

$$z = \begin{cases} (z_B - z_C)(2 - \tau)^3 + z_C, & 1 \le T \le 2; \text{ for BC,} \\ (z_D - z_C)(T - 2)^3 + z_C, & 2 \le T \le 3 \text{ for CD.} \end{cases}$$

Boundary Test Points. Sixteen points equally spaced, in steps of 0.25, starting from A.

Numerical Results.

BKM/MB : N_{opt}= 13, $E_{13} = 5.865 \times 10^{-3}$, $R_{13} = 1.15608265313$.
RM/MB : $E_{13} = 5.865 \times 10^{-3}$, $R_{13} = 1{,}15608265325$.
BKM/AB : $N_{opt} = 16$, $E_{16} = 5.368 \times 10^{-6}$, $R_{16} = 1.15601515324$.
RM/AB : $E_{16} = 5.285 \times 10^{-6}$, $R_{16} = 1.15601515316$.

In table 5.1 we present the detailed execution times obtained by applying the above four methods, i.e. the BKM/MB and RM/MB with n = 13 and BKM/AB and RM/AB with n = 16. These results indicate that, for the same set of basis functions, the execution time of the RM is comparable to that of the BKM although, in general, the BKM/AB turns out to be slightly faster than the RM/AB. This can be explained by the fact that the singular functions used in the RM/AB involve the additional constants c_j and d_k. These observations regarding execution times do not agree with those of Gaier [10, p. 154], The experiments of [I0], preformed by using a monomial basis, indicate that the RM is considerably faster than the BKM. The reason for this variance could be due to the differences

between the computing equipment available in 1964 and the present time.

	Execution times in secs			
	BKM/MB	RM/MB	BKM/AB	RM/AB
Evaluation of Inner Products	0. 3 75	0. 178	0.429	0.496
Orthonormalization Process	0.005	-	0.010	-
Solution of Linear System	-	0.001	-	0.002
Total Time	0.212	0.204	0.497	0.529

TABLE 5.1

Example 5.2 The region shown in Figure 5.2

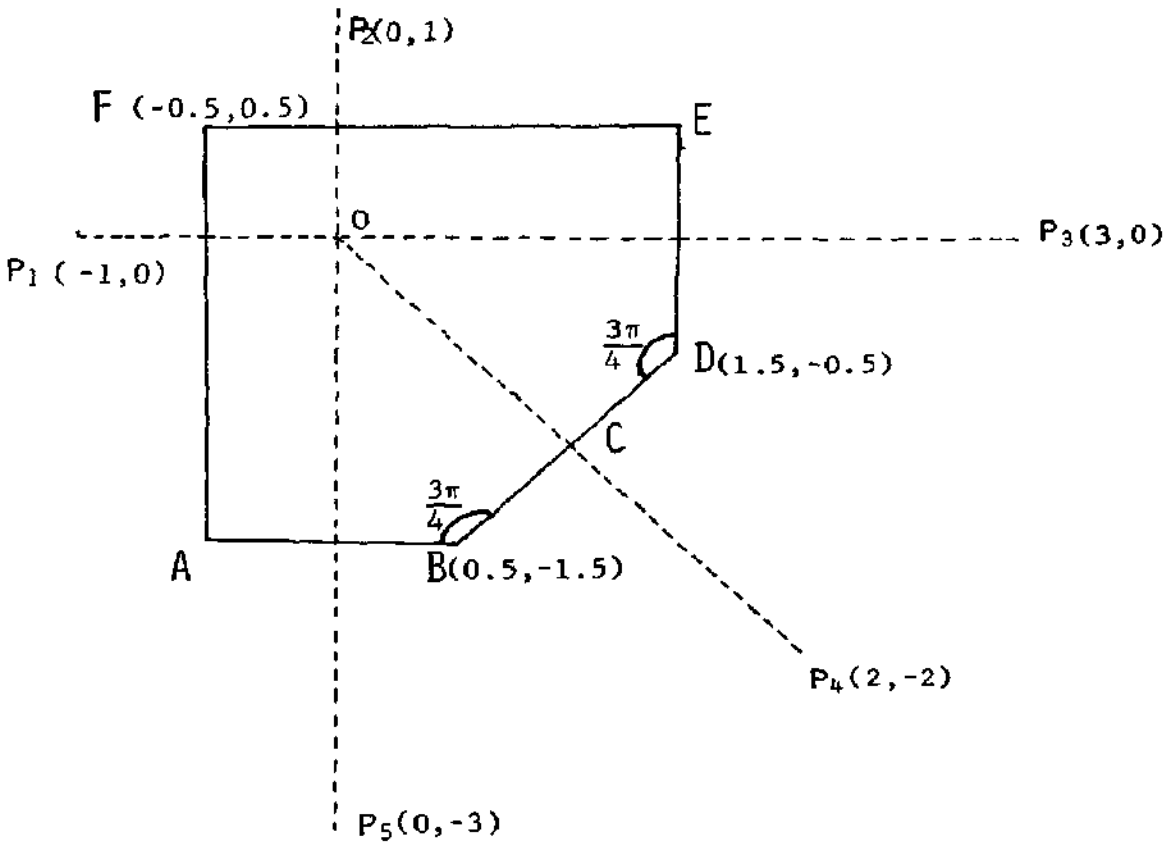

FIGURE 5.2

Augmented Basis. The following singular functions corresponding respectively to the poles at the points p_j, $j = 1,2,3,4,5$ and the branch points singularities at the corners B and D are used:

$$-pj \;/\; (z-p_j)^2 + c_j, \quad j = 1,2,3,4,5$$

and

$$\frac{4k}{3}(z-z_B)^{\frac{4k}{3}-1} - d_{1k}, \quad \frac{4k}{3}(z-z_D)^{\frac{4k}{3}-1} - d_{2k}; \; k = 1,2,$$

where in the BKM/AB, $c_i = 0$, $d_{1k} = d_{2k} = 0$

and in the RM/AB$_2$ $c_j = 1/p_j$, $d_{1k} = \left\{ 4k\,(-z_B)^{\frac{4k}{3}-1} \right\} / 3$, $d2k = \left\{ 4k\,(-z_D)^{\frac{4k}{3}-1} \right\} / 3$.

Quadrature. Gauss-legendre formula with 16 points along AB, BC,....,FA.

In order to perform the integration accurately we choose the parametric representations of AB, BC, CD, DE to be

$$z = \begin{cases} (z_A - z_B)\,(1-\tau)^3 + z_B, & 0 \le \tau \le 1; \quad \text{for AB,} \\ (z_C - z_B)\,(\tau-1)^3 + z_B, & 1 \le \tau \le 2; \quad \text{for BC,} \\ (z_C - z_D)\,(3-\tau)^3 + z_D, & 2 \le \tau \le 3; \quad \text{for CD,} \\ (z_D - z_E)\,(\tau-3)^3 + z_D, & 3 \le \tau \le 4; \quad \text{for DE,} \end{cases}$$

Boundary Test Points. Twenty four points equally spaced, in steps of 0.25, starting from A.

Numerical Results.

BKM/MB : $N_{opt} = 15$, $E_{15} = 5.041 \times 10^{-3}$, $R_{15} = 0.690478428461$.
RM/MB : $E_{15} = 5.116 \times 10^{-3}$, $R_{15} = 0.690476981221$.
BKM/AB : $N_{opt} = 19$, $E_{19} = 8.680 \times 10^{-7}$, $R_{19} = 0.690412899521$.
RM/AB : $E_{19} = 9.245 \times 10^{-7}$, $R_{19} = 0.690412899521$.

Example 5.3 The region shown in Figure 5.3. In this, EA is inclined at an angle of $37\pi/4$ to the real axis, and AB is an arc of the circle with centre (-1, 1.4) and radius 0.8.

Augmented Basis. The following singular functions corresponding to the poles at the points p_j; $j = 1,2,3,4$ are used:

$-p_j/(z - p_j)^2 + c_j$; $j = 1,2,3,4$, where in the BKM/AB, $c_j = 0$ and the RM/AB, $c_i = 1/p_i$.

Quadrature. Gauss-Legendre formula with 16 points along AB, BC,....,FA.

Boundary Test Points. Twenty four points. On the straight line segments these points are equally spaced, in steps of 0,25, starting from B.

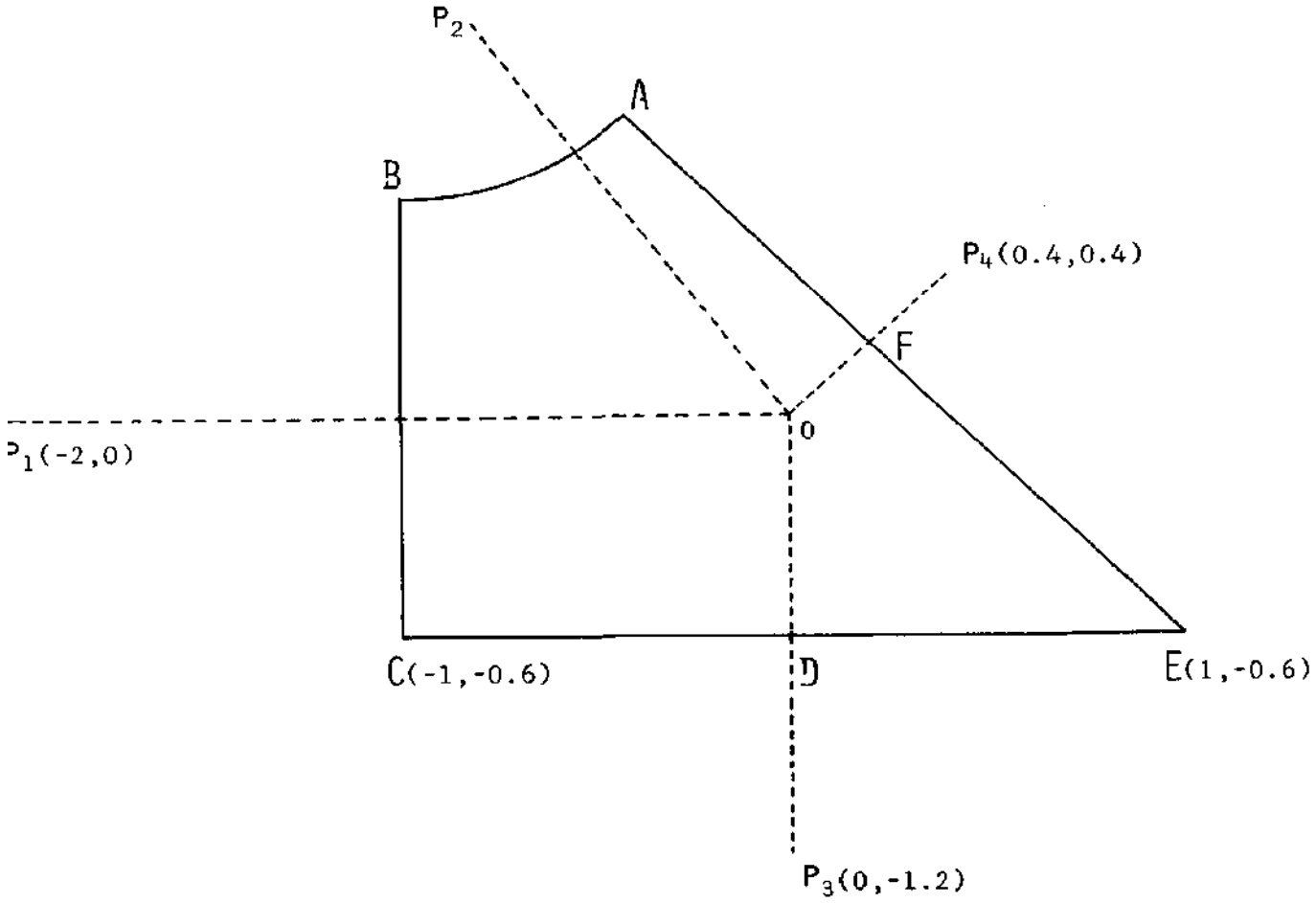

(The point p_2 is the inverse point of the orgin with respect to the arc AB.)

FIGURE 5.3

Numerical Results.

BKM/AB : $N_{opt} = 25$, $E_{25} = 1.468 \times 10^{-7}$, $R_{25} = 0.478807443760$.

RM/AB : $E_{25} = 1.011 \times 30^{-7}$, $R_{25} = 0.478807443760$.

Example 5.4 The region shown in Figure 5.4

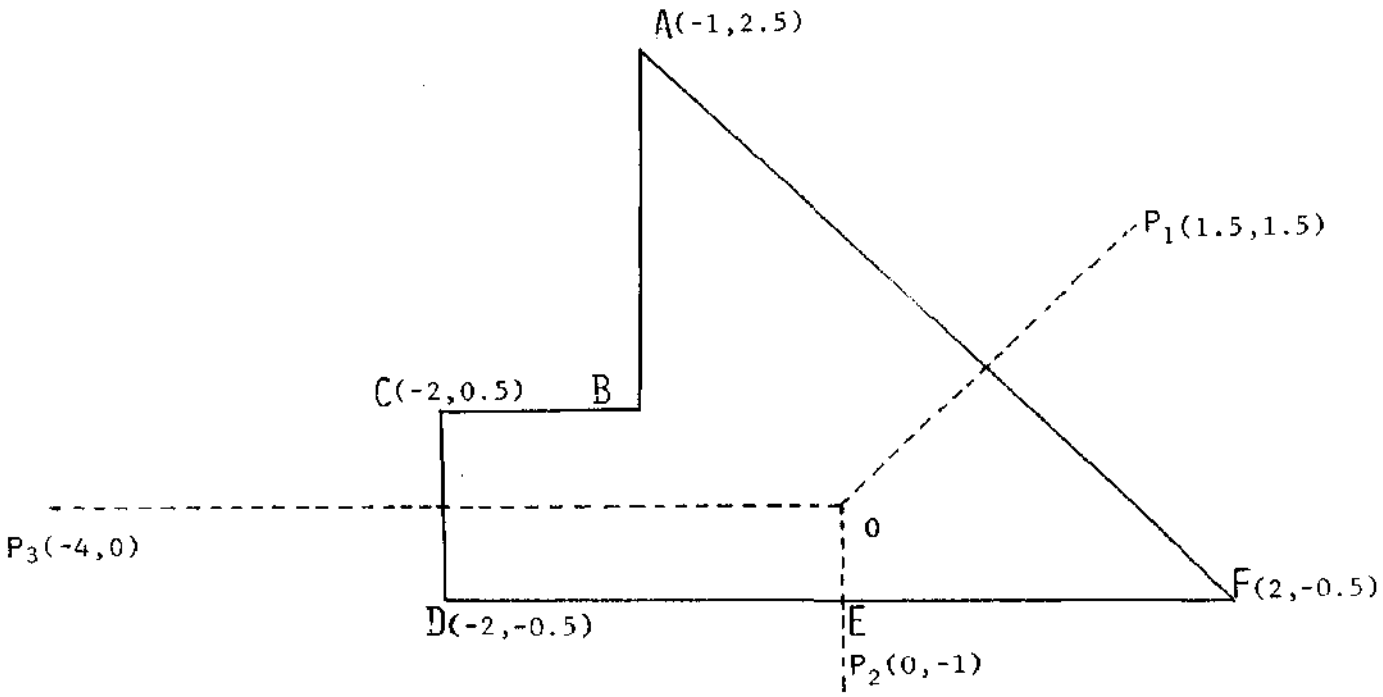

FIGURE 5.4

Augmented Basis. The following singular functions corresponding respectively to the poles at the points p_j; j = 1,2,3 and the branch point singularity at the corner B are used:

$-p_j / (z - p_j)^2 + c_j$; j = 1,2,3 and $\frac{2k}{3}(z-z_B)^{\frac{2k}{3}-1} - d_k$; k = 1,2,4,5,7,

where in the BKM/AB $c_j = 0$, $d_k = 0$ and in the RM/AB $c_j = 1/p_j$,

$$d_k = \left\{ 2k\,(z-z_B)^{\frac{2k}{3}-1} \right\} / 3.$$

Quadrature. Gauss-Legendre formula with 16 points along AB, BC,....,FA. In order to perform the integration accurately we choose the parametric representations of AB, BC to be

$$z = \begin{cases} (z_A - z_B)(1 - \tau)^3 + z_B, & 0 \le \tau \le 1; \quad \text{for AB,} \\ (z_C - z_B)(\tau - 1)^3 + z_B, & 1 \le \tau \le 2; \quad \text{for BC.} \end{cases}$$

Boundary Test Points. Twenty four points equally spaced, in steps of 0.25, starting from A.

Numerical Results.

BKM/AB : $N_{opt} = 20$, $E_{20} = 2.171 \times 10^{-5}$, $R_{20} = 0.829851089401$.
RM/AB : $E_{20} = 1.804 \times 10^{-5}$, $R_{20} = 0.829851090640$.

6. Applications.

All the examples considered in this section involve the conformal mapping of the domain $\Omega \in$ z-plane onto the rectangle

$$\Omega' = \{(\xi, \eta) : 0 < \xi < 1, \quad 0 < \eta < H\} , \tag{6.1}$$

in the w' -plane ($w' = \xi + i\eta$), so that four specified points $A_i \in \partial\Omega$, $i = 1,2,3,4$, on the boundary of Ω, are mapped respectively onto the four vertices $(0,0)$, $(0,H)$, $(1,H)$ and $(1,0)$ of Ω'. This mapping can be performed by using the subroutine CTM1 of Papamichael and Sideridis [22], after first transforming Ω onto the upper half w-plane by means of the tranformation

$$w = T(z) = i\{1 + F(z)\} / \{1 - F(z)\} , \tag{6.2}$$

where F is the function mapping Ω onto the unit disc; see Figure 6.1. The subroutine CTM1 maps the upper half-plane onto the rectangle Ω' by means of a bilinear and a simple Schwarz-Christoffel transformations. Its main computational requirement is the calculation of two incomplete elliptic integrals of the first kind for each transformed point; see [23] and [24], In particular, if the exact mapping function F is known then (6.2), in conduction with the CTMl, produces essentially the exact conformal map of Ω onto Ω' . If F is not known analytically then an approximate conformal map is obtained by replacing (6.2) by

$$w = \tilde{T}(z) = i\{1 + \tilde{F}(z)\} / \{1 - \tilde{F}(z)\} , \tag{6.3}$$

where $\tilde{F}$ is an approximation to F.

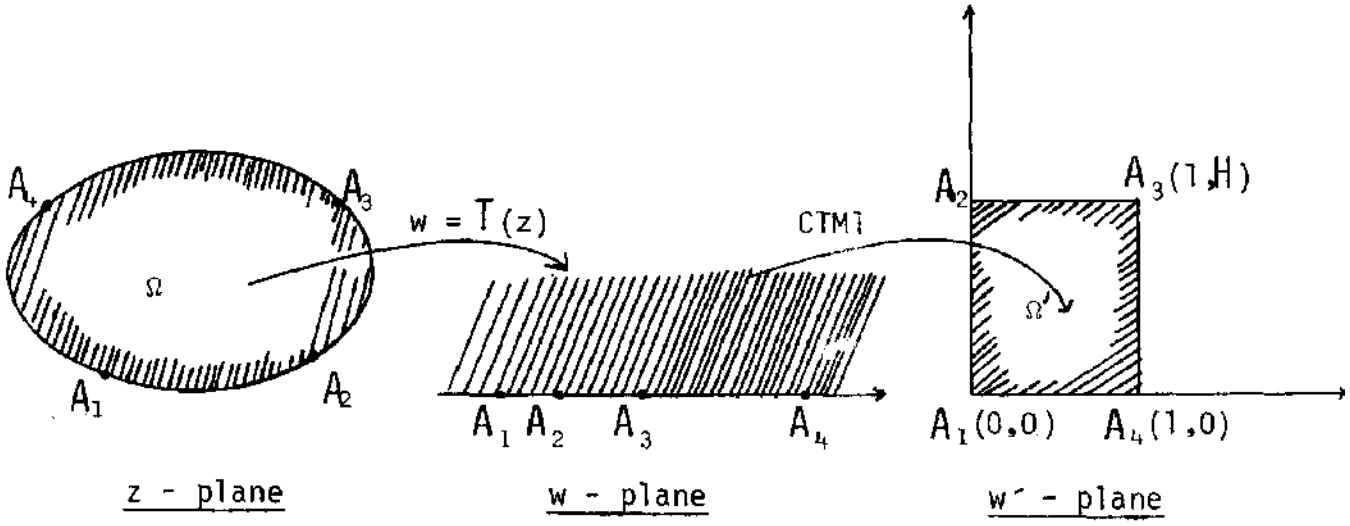

FIGURE 6.1

The above procedure for mapping Ω onto Ω′ forms the basis of a conformal transformation method for the numerical solution of a class of elliptic boundary value problems. This method is discussed fully in Papamichael and Sideridis [23] and, for this reason, its application is not considered here. Instead, we consider a number of examples which require only the computation of the height H of the rectangle Ω'. This is a particularly simple computation, since H is given by the formula

$$H = K\{(1 - k^2\}^{1/2} / K(k) \quad , \tag{6.4}$$

where K(k) is the complete elliptic integral of the first kind with modulus

$$k = d^{-\frac{1}{2}} \quad , \quad d = \left\{\left(\frac{T(z_4) - T(z_2)}{T(z_4) - T(z_1)}\right)\left(\frac{T(z_3) - T(z_1)}{T(z_3) - T(z_2)}\right)\right\} \tag{6.5}$$

In (6.5), $T(z_i)$ are the images of the points $A_i = z_i$ in the w-plane, i.e. d is the cross-ratio of these images; see e.g. [5], [12] and [22].
It follows from (6.4) and (6.5) that, for a given domain Ω, the height H of the rectangle Ω' is determined completely by the position of the four boundary points A_i . We indicate this by writing

$$H = H\{A_1, A_2, A_3, A_4\} \quad . \tag{6.6}$$

In fact H is the so—called conformal module of the quadrilateral defined by the points A_i , i = 1,2,3,4; see Gaier [11], [12], This domain functional has many practical applications and some of these are described briefly below.

Consider a thin resistor in the shape of ft, cut from a sheet of material of uniform resistivity. Assume that constant voltages are applied to the boundary segments A_1A_2 and A_3A_4 whilst the remainder of $\partial\Omega$ is insulated. Then 1/H, the reciprocal of the conformal module (6.6), gives the geometric resistance of the resistor; see e.g. Bowman [5,p.63] and Trefethen [30]. The conformal module is also closely related to the capacitance C between A_1A_2 and A_3A_4. This is defined as the charge on A_1A_2 when A_3A_4 is at unit potential and the remainder of $\partial\Omega$ is at zero potential; see e.g. Campbell [7]. If H is the conformal module (6.6) then it is shown in Gaier [13] that

$$C = \frac{2}{\pi^2} \sum_{r=1}^{\infty} \{(2r-1)\sinh[2r-1)\,\pi/H]\}^{-1} \qquad (6.7)$$

The final application considered here concerns the computation of the moduli of certain doubly-connected domains. Let the bounded simply-connected domain ft lie in the upper half z-plane and assume that it is partly bounded by two line segments A_1A_2 and A_3A_4 on Re{z}, where A_1A_2 A_3A_4 are the only boundary segments on the real axis; see Figure 6.2(a). Let G be the doubly-connected domain obtained by reflecting Ω about the real axis. Then, 0 can be mapped conformally onto the circular annulus $1 < |w''| < M$ in the w'-plane, where the radius M of the outer circle is called the modulus of G. This conformal mapping of G has many practical applications, and in these the value of the modulus M is often of special significance; see e.g. Lewis [18] where M is simply related to the flow parameter of a hydrostatic oil bearing. Referring to the domain ft of Figure 6.2(a), let $H = H\{A_1,A_2,A_3,A_4\}$ be the conformal module of the quadrilateral defined by the four points A.; i = 1,2,3,4. Then, the

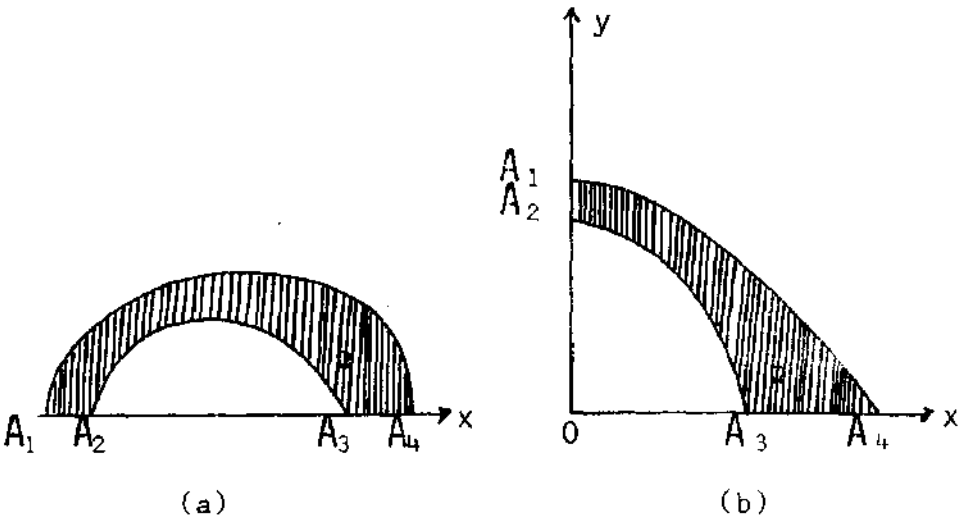

FIGURE 6.2

modulus M of G Is related to H by

$$M = \exp\{\pi H\} \quad ; \tag{6.8}$$

see e.g. Gaier [11,p.188], The result (6.8) can be deduced from the observation that the conformal map

$$w^{\sim} = \exp\{\pi(iw' + H)\} \quad , \tag{6.9}$$

transforms the rectangle Ω' of Figure 6.1 onto the domain

$$\Omega'' = \{re^{i\theta} : 1<r<M = \exp\pi H\,,\ 0<\theta<\Pi\} \quad ,$$

so that the corners A_i; i = 1,2,3,4 of Ω' are mapped respectively onto the points (M,0), (1,0), (-1,0) and (-M,0). Similar results hold if the doubly-connected domain consists of more than two identical and symmetrical parts. For example, if G is obtained through the reflexion of the domain Ω of Figure 6.2(b) about the real and imaginary axes then clearly

$$M = \exp\{\pi H/2\} \quad , \tag{6.10}$$

In the examples presented below we use the approximate conformal maps obtained in Section 5 to compute approximations to various conformal modules and hence, by means of (6.8), approximations to the moduli of certain doubly connected domains.

Example 6.1. Let G be the square frame

$$G = \{(x,y): 0.5<|x|<1,|y|<1\} \cup \{(x,y): |x|<1,0.5<|y|<1\},$$

illustrated in Figure 6.3.

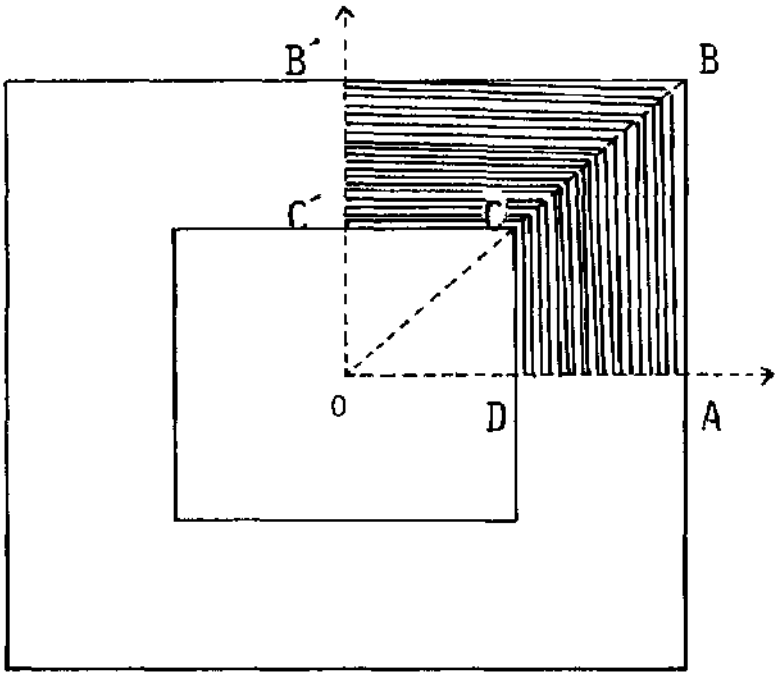

FIGURE 6.3

We determine two approximations to the modulus M of G, by first computing approximations $\tilde{H}_1$, $\tilde{H}_2$ to the conformal modules

$$H_1 = H_1\{B', C', A\}, \qquad H_2 - H_2\{B,C,D,A\},$$

corresponding respectively to the L-shaped domain Ω_1 bounded by ABB'C 'CDA and to the quadrilateral Ω_2 bounded by ABCDA.

In the case of Ω_1, the exact value of the cross-ratio d corresponding to H_1 can be derived from the results of Gaier [11, p. 189], which give

$$d = (7\sqrt{3} + 12)/24.$$

Hence, the exact value of H_1 can be determined by means of (6.4)-(6.5). In this way we find that, correct to six significant figures,

$$H_1 = 0.390850 \text{ and } H_2 = 2H_1 = 0.781701.$$

In computing $\tilde{H}_1$ and $\tilde{H}_2$, the approximations $\tilde{F}$ used in (6.3) for the mapping of Ω_1 and Ω_2 are as follows. In the case of Ω_1, $\tilde{F}$ is the BKM/AB approximation which is given explicitely in [21,Ex.2.3]. In the case of Ω_2, $\tilde{F}$ is the BKM/AB approximation obtained in Example 5.1, The numerical results obtained are

$$\tilde{H}_1 = 0.390840 \quad \text{and} \quad \tilde{H}_2 = 0.781708.$$

These give respectively the approximations

$$\tilde{M}_1 = \exp\{\pi \tilde{H}_1/2\} = 1.847680,$$

and

$$\tilde{M}_2 = \exp\{\pi \tilde{H}_2/4\} = 1.847719,$$

to the modulus M of G. The exact value of M, correct to seven significant figures, is

$$M = \exp\{\pi H_1/2\} = \exp\{\pi H_2/4\} = 1.847709.$$

Example 6.2. Let G be the doubly—connected domain illustrated in Figure 6.4. The outer boundary of G is a square of length 4 whose sides are parallel to the co-ordinate axes. The inner boundary is a concentric square, of length $\sqrt{2}$, whose sides are rotated through 45 with respect to the axes,

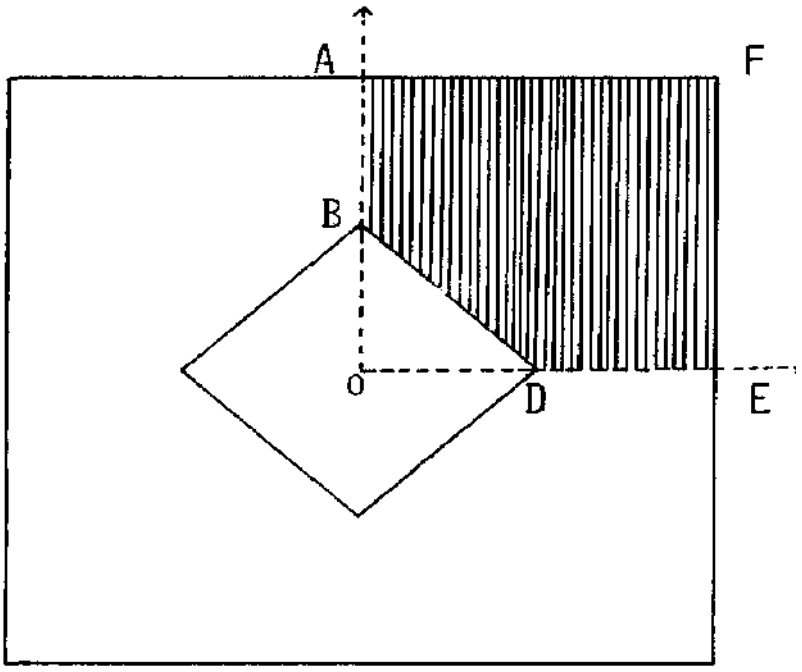

FIGURE 6.4

To determine an approximation $\tilde{M}$ to the modulus M of G, we first compute an approximation $\tilde{H}$ to the conformal module

$$H = H\{A,B,D,E\} ,$$

corresponding to the domain Ω bounded by ABUEFA, i.e. Ω is the domain of Example 5.2. For the computation of $\tilde{H}$, we take in (6.3) $\tilde{F}$ to be the BKM/AB approximation obtained in Example 5.2. In this way we find

$$\tilde{H} = 0.602630$$

and

$$\tilde{M} = \exp\{\pi\tilde{H}/2\} = 2.576958, \tag{6.11}$$

In this case the exact value of M is not known. However, the approximation (6.11) should be compared with the value 2.578411, obtained by an integral equation method in Richardson and Wilson [26,p.316], and with the result

$$2.57623<M<2.57806,$$

established in Gaier [11,p.192], by a finite difference method based on a variational property of the Dirichlet integral of Ω.

Example 6.3. Let G be the doubly connected domain

$$G = \{(x,y): |x|<1,|y|<1\} \cap \{z : |z|>0.4\} ,$$

illustrated in Figure 6.5.

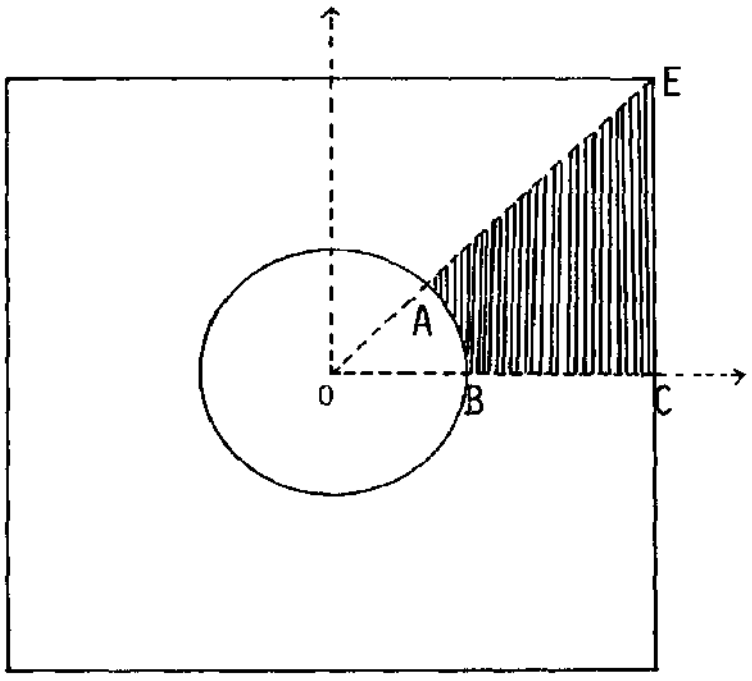

FIGURE 6.5

Let Ω be the domain bounded by the straight lines BC, CE, EA, and the circular arc AB, i.e. Ω is the domain of Example 5.3. We compute the approximation $\tilde{H}$ to the conformal module

$$H = H\{E,A,B,C\}$$

of Ω, by taking in (6.3) $\tilde{F}$ to be the BKM/AB approximation obtained in Example 5.3. In this way we find

$$\tilde{H} = 1.263102.$$

Hence,

$$\tilde{M} - \exp\{\pi\tilde{H}/4\} = 2.696725,$$

gives an approximation to the modulus M of G. This approximation $\tilde{M}$ should be compared with the values 2.69861 and 2.69677 obtained in Gaier [14], by using respectively the integral equation methods of Symm [29] and Hayes et al [15], and the value 2.696724 obtained by using a variational method for doubly-connected domains; see [10,p.2491. As is pointed out in [14], this last value is probably correct to five decimal places.

Example 6.4. Let G be the doubly-connected domain illustrated in Figure 6.6. This domain is the intersection of the square domain

$$\{(x,y): |x|<4,|y|<4\} ,$$

with the complement of the domain

$$\{(x,y): |x|<3,|y[<1\} \cup \{(x,y): |x|<1,|y|<3\} .$$

Let Ω be the domain bounded by ABCDFA, i.e. Ω is the domain of Example 5.4. We compute the approximation $\tilde{H}$ to the conformal module

$$H = H\{F,A,C,D\}$$

of Ω, by taking in (6.3) $\tilde{F}$ to be the BKM/AB approxiamtion of Example 5.4. In this way we find

$$\tilde{H} = 0.497750.$$

Hence,

$$M = \exp\{\pi\tilde{H}/4\} = 1.478358$$

is an approximation to the donulus M of G. This approximation should be compared with the value 1.478296 which we obtained by using a method

based on the variational technique for doubly-connected domains described in [10,p.249].

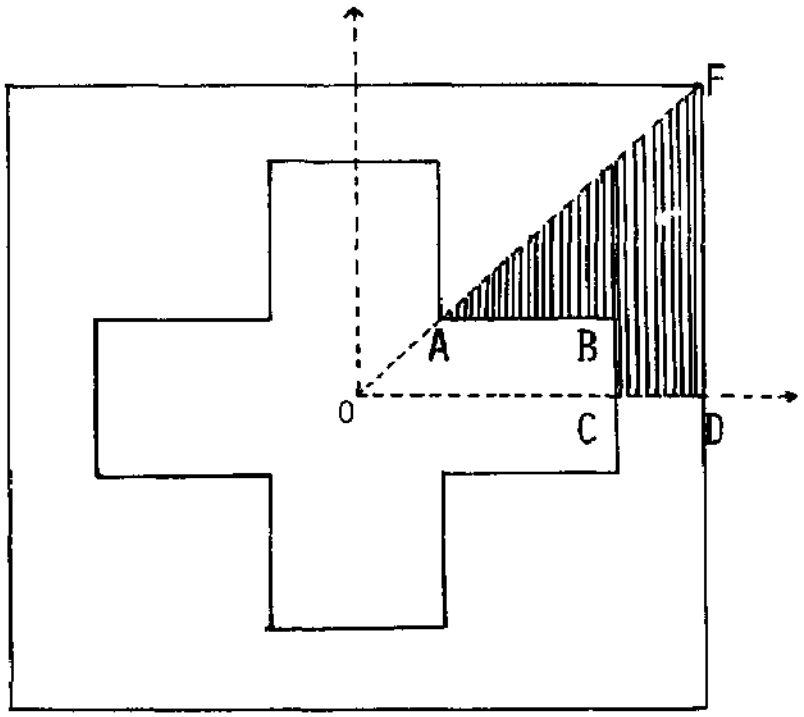

FIGURE 6,6

Discussion

The numerical examples of Section 5 indicate clearly that the RM produces results of comparable accuracy to those obtained by the BKM. Like the BKM, the RM with a suitable augmented basis is an extremely efficient method for the numerical confortnal mapping of simply—connected domains. Regarding conputational effort, our experiments show that for the same number of basis functions the computation time of the RM is comparable to that of the BKM. However, the RM involves the solution of a new (n+m-1) x (n+m-1) complex linear system, each time that the number n of basis functions is increased to n+m. This is clearly a drawback of the method.

The procedure described in Section 6, for mapping a given simply-connected domain onto a rectangle, has a number of practical applications. In

particular, as the examples of Section 6 indicate, this procedure leads to an efficient method for determining accurate approximations to the moduli of a class of doubly—connected domains.

REFERENCES

[1] Aronzajn, N.n (1950) Theory of Reproducing Kernels, Trans. Amer. Math. Soc. 68, 337-404.

[2] Bergman, S., (1970) The Kernel Function and Conformal Mapping, Math, Surveys, No. 5, Amer. Math. Soc. Providence, R.I. (Second Edition).

[3] Bergman, S., and J.G. Herriot (1961) Application of the Method of the Kernel Function For Solving Boundary Value Problems, Numer. Math. 3 209-225.

[4] Bieberbach, L., (1914) Zur Theorie and Praxis der konformen Abbildung, Rend. Circ. Mat. Palermo 38, 98-112.

[5] Bowman, F., (1953) Introduction to Elliptic Functions, London: English University Press.

[6] Burbea, J., (1970) A Procedure for Conformal Maps of Simply-Connected Domains by Using the Bergman Function, Math. Comp. 24, 821-829.

[7] Campbell, J.B., (1975) Finite Difference Techniques for Ring Capacitors, J. Eng. Math. 9, 21-28.

[8] Copson, E.T., (1975) Partial Differential Equations, London: Cambridge University Press.

[9] Davis, P.J., and R. Rabinowitz, (1961) Advances in Orthonormalizing Computation, In Advances in Computers, Vol. 2 (Ed. Franz L. Alt), p.55, London and New York: Academic Press.

[10] Gaier, D., (1964) Konstruktive Methoden der konformen Abbildung, Berlin: Springer-Verlag.

[11] Gaier, D., (1972) Ermittlung des konformen Modulus von Vierecken mit Differenzemmethoden, Numer . Math. 19, 179-194.

[12] Gaier, D., (1974) Determination of Conformal Modules of Ring Domains and Quadrilaterals, Lecture Notes in Mathematics No. 399, pp. 180-188, New York: Springer-Verlag.

[13] Gaier, D., (1979) Capacitance and the Conformal Module of Quadrilaterals, J. Math. Analysis and Applications 70, 236-239,

[I4] Gaier, D., (1980) Das logarithmische Potential und die konforme Abbildung mehrfach zusammentiangender Gebiete. To appear in a Vol. dedicated to the 150th birthday of E.B. Christoffel.

[15] Hayes, J.K., D.K. Kahaner, and R.G. Kellner (1972) An Improved Method for Numerical Conformal Mapping, Math. Comp. 29, 512-521.

[16] Lehman, R.S., (1957) Development of the Mapping Function at an Analytic Corner, Pacific J. Math. 7 , 1437-1449.

[17] Levin, D., N. Papamichael, and A. Sideridis (1978) The Bergman Kernel Method for the Numerical Conformal Mapping of Simply Connected Domains, J, Inst. Maths Applies 22, 171-187.

[18] Lewis, G.K., (1966) Flow and Load Parameters of Hydrostatic Oil Bearing for Several Port Shapes, J. Mech. Eng. Sci. 8, 173-184,

[19] Markushevich, (1967) Theory of Functions of a Complex Variable, Vol III, Englewood Cliffs, N.J: Prentice-Hall,

[20] Nehari, Z., (1952) Conformal Mapping, New-York: McGraw-Hill.

[21] Papamichael, N., and A. Sideridis (1977) Formulae for the Approximate Conformal Mapping of Some Simply Connected Domains, Technical Reprot TR/72, Dept. of Maths, Brunel University.

[22] Papamichael, N., and A, Sideridis (1979) Subroutine CTM1, Technical Report TR/89, Dept. of Maths, Brunel University.

[23] Papamichael, N., and A. Sideridis (1979) The Use of Conformal Transformations for the Numerical Solution of Elliptic Boundary Value Problems with Boundary Singularities, J. Inst, Maths Applies, 23, 73-88.

[24] Papamichael, N., and G.T. Symm (1975) Numerical Techniques for Two-Dimensional Laplacian Problems, Comp. Maths Appl. Mech. Engng 6, 175-194.

[25] Pryce, J.D. (1973) Basic Methods of Linear Functional Analysis, London: Hutchinson University Library.

[26] Richardson, M.K. and H.B. Wilson, (1967) A Numerical Method for the Conformal Mapping of Finite Doubly Connected Domains, Developments in Theoretical and Applied Mechanics, 3, 305-321.

[27] Smirnov, V.I. and N.A. Lebedev (1968) Functions of a Complex Variable, London: Iliffe.

[28] Švecova, H., (1970) On the Bauer's Scaled Condition Number of Matrices Arising from Approximate Conformal Mapping, Numer. Math. 14, 495-507.

[29] Symm, G.T. (1969) Conformal Mapping of Doubly-Connected Domains, Numer. Math. 13, 448-457.

[30] Trefethen, L.N. (1980) Design of Polygonal Resistors by means of the Schwarz-Christoffel transformation. To appear in: Solid State Technology.

[31] Walsh, J.L. (1969) Interpolation and Approximation by Rational Functions in the Complex Domain" Amer. Math. Soc. Coll. Pub. XX 5th ed.

[32] Yosida, K. (1968) Functional Analysis, Berlin: Springer-Verlag.